

## Spectroscopy of $A0^+ \leftarrow X0^+$ and $B1 \leftarrow X0^+$ transitions in CdKr

M. Czajkowski, R. Bobkowski, and L. Krause

*Department of Physics, University of Windsor, Windsor, Ontario, Canada N9B 3P4*

(Received 2 April 1991)

Excitation spectra of the CdKr excimer were produced in a molecular beam employing free-jet supersonic expansion, crossed with a pulsed dye-laser beam. Bands arising from  $B1 \leftarrow X0^+$  and  $A0^+ \leftarrow X0^+$  vibronic transitions were analyzed, yielding spectroscopic constants for the three states. Computer simulations of the bands yielded relative values of  $r_e$ , the equilibrium internuclear separations. Potential-energy curves constructed on the basis of the data and of the Morse potential provided a useful comparison with theoretically calculated curves.

PACS number(s): 33.20.Lg, 33.50.Dq

### I. INTRODUCTION

We have recently reported the results of experiments on the spectroscopy of  $A0^+ \leftarrow X0^+$  and  $B1 \leftarrow X0^+$  transitions in CdNe and CdAr van der Waals molecules, carried out in a supersonic expansion beam crossed with a laser beam [1]. There appears to be continuing interest in experimental studies of group-IIb-metal-noble-gas van der Waals molecules [2,3], which permit a direct comparison with calculations of the respective molecular potentials [4] and potential-energy (PE) curves [5]. In addition to checks on theoretical potentials and *ab initio* calculations, spectroscopic studies of van der Waals molecules provide important and useful information on dimer-monomer collisions leading to energy transfer, on various relaxation phenomena involving the gas-phase molecules, molecular dynamics, and bulk properties of gases [6]. We now report on the spectroscopy of the CdKr molecule which we studied by methods of laser-induced fluorescence (LIF) in an expansion beam. Although the CdKr spectrum has been investigated previously [7,8], we have been able to effect a significant improvement in the reliability of the resulting molecular constants and carry out a comparison with theoretical calculations [9]. The PE curves for the CdKr van der Waals molecule, which are not generally known, have been calculated *ab initio* by Czuchaj and Sienkiewicz [9], who used the Baylis [4] molecular potentials. Here we make a comparison between the calculated PE curves and those derived from experimental data.

### II. EXPERIMENTAL PROCEDURE

The apparatus and experimental procedure have been described elsewhere [1,10]. The spectra were excited in an evacuated expansion chamber into which Cd atoms seeded in a mixture of Kr and Ne as a carrier gas were injected through a nozzle constituting part of the beam source. Certain modifications were made to the source, which were crucial to the success of the experiments. Both the oven chamber and the nozzle were fabricated of molybdenum, with the nozzle having a diameter 150  $\mu\text{m}$  and a channel length 350  $\mu\text{m}$ . The nozzle was connected

to the oven chamber by a threaded coupling which was sealed with a soft-iron wedge-shaped washer squeezed between two polished flat surfaces. This arrangement was found to be free of leaks, prevented clogging of the nozzle orifice and could be operated at temperatures up to 1000 K, which corresponded to a Cd vapor pressure of 580 Torr at which both Cd<sub>2</sub> and CdKr molecules could be produced in the jet with relative ease. The carrier gas consisted of 90 vol. % Ne and 10 vol. % Kr, since we found Ne to be very efficient in cooling the molecules in the beam and to have a relatively small propensity to form CdNe molecules whose spectra, lying on the wing on the Cd resonance line, are well separated from the CdKr spectra. Ne turned out to be a much more satisfactory carrier gas than He [10].

The molecules in the beam were irradiated with the second-harmonic output of an in-house-built dye laser operated with a  $5.8 \times 10^{-4} M$  solution of 4-dicyanomethylene-2-methyl-6-(p-dimethylaminostyryl)-4H-pyran (DCM) in dimethyl sulphoxide and pumped with the second harmonic of a Q-switched neodymium-doped yttrium aluminum garnet (Nd:YAG) laser. The wavelength calibration of the dye laser was frequently verified against a Fizeau-wedge wave meter [11], and the spectral linewidth of its output was found to be approximately 0.2  $\text{cm}^{-1}$ , using a Fabry-Pérot étalon. The fluorescence spectrum was monitored at right angles to the plane containing the crossed atomic and laser beams and was detected with a Schlumberger EMR-541-N-03-14 photomultiplier (PM) tube which had its peak sensitivity in the uv and blue spectral regions and was insensitive to radiation of wavelength longer than 6200 Å [10]. The photomultiplier signal was registered with a EG&G 162/166 boxcar integrator and was stored in a microcomputer which also controlled the scanning mechanism of the dye laser.

The beam source was operated at a temperature of about 760 K, which corresponded to a Cd vapor pressure of about 12 Torr. We used a backing pressure of 11.2 atm of the Ne+Kr mixture, at which the frequency of the collisions in the expanding beam was expected to be relatively high [12], and consequently, we performed the experiments using a moderately high value of the  $X/D$

parameter ( $X/D = 65$ ), where  $X$  is the distance between the nozzle and the excitation region ( $\sim 1$  cm) and  $D$  is the nozzle diameter ( $150 \mu\text{m}$ ). Lower carrier-gas pressures resulted in the production of insufficient CdKr molecules. On the other hand, an increase in  $X$  to 1.5–2.0 cm and an improvement of the cooling efficiency [12] resulted in the rapid decline of the PM signal as the density of the molecules in the beam decreased. The mechanical and thermal stability of the whole apparatus was very satisfactory as was the reproducibility of the data.

### III. RESULTS AND DISCUSSION

#### A. The $B1 \leftarrow X0^+$ excitation spectrum

Figure 1 shows a trace of an excitation spectrum which consists of ten vibronic bands in the region 3250.8–3256.7 Å, and arises from  $B1 \leftarrow X0^+$  transitions. The spectrum, in which it is possible to identify more vibrational bands than could be done previously [7], includes a  $v'$  progression as well as two “hot bands” arising from states with  $v''=1$ , and the frequencies of the components are listed in Table I. The trace also contains peaks belonging to a  $v'$  progression in the  $\text{Cd}_2$  spectrum [10]. Figure 2 shows a Birge-Sponer plot of  $G(v' + \frac{1}{2})$  against  $v'$  for the components of the  $v'$  progression, which exhibits a considerable deviation from linearity, indicating that the PE curve for the  $B1$  state cannot be represented by the Morse potential [13,14] and the Morse approximation cannot be used to evaluate  $D'_e$ . The plot, extrapolated to  $v'=0$ , yielded  $\omega'_e$ . An extrapolation of the plot to  $\Delta G=0$  intersects the  $v'$  axis at  $v'=9$ , which corresponds to the actual dissociation limit.  $D'_0$  is directly obtainable from the area under the Birge-Sponer plot, and the area under the extrapolated experimental plot yielded  $D'_0(B1) = 55.5 \pm 0.3 \text{ cm}^{-1}$ . It is also sometimes useful to plot  $\Delta G(v' + \frac{1}{2})$  against the total vibrational energy  $G(v')$  [14]. As may be seen in Fig. 3, such a plot is

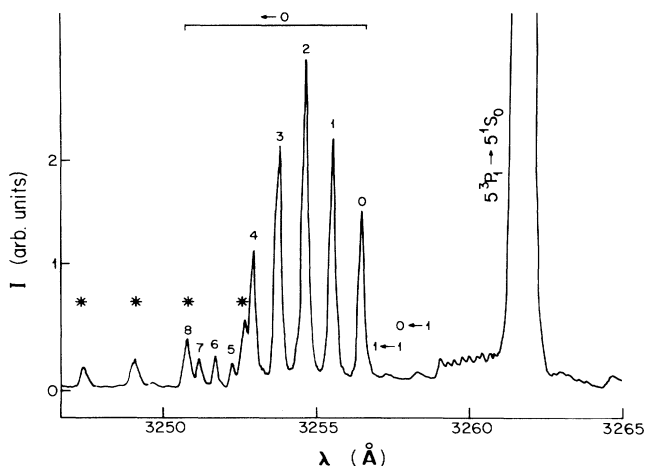


FIG. 1.  $B1 \leftarrow X0^+$  excitation spectrum of CdKr, showing  $v' \leftarrow v''$  assignments. The spectrum contains two ( $1 \leftarrow 1$  and  $0 \leftarrow 1$ ) “hot bands.”  $T = 760 \text{ K}$ ,  $P_0 = 11.2 \text{ atm}$  (Kr+Ne),  $X/D = 65$ . \*, components of the  $\text{Cd}_2$  spectrum.

TABLE I. Frequencies of  $B1 \leftarrow X0^+$  vibrational bands.

$v' \leftarrow v''$	$\bar{\nu}$ ( $\text{cm}^{-1}$ )	$\Delta G(v')$ ( $\text{cm}^{-1}$ )
0 ← 0	30 706.1	8.9
1 ← 0	30 715.0	8.5
2 ← 0	30 723.5	8.1
3 ← 0	30 731.6	7.7
4 ← 0	30 739.3	7.0
5 ← 0	30 746.4	6.3
6 ← 0	30 752.6	5.0
7 ← 0	30 757.6	3.3
8 ← 0	30 760.9	1.1
9 ← 0	30 762.0	
0 ← 1	30 689.0	
1 ← 1	30 689.0	

of roughly parabolic form and its extrapolated intercept on the  $G(v')$  axis yields directly the dissociation energy  $D'_0(B1) = 56.3 \pm 0.3 \text{ cm}^{-1}$ . The two values are in good agreement with one another and give the average  $D'_0(B1) = 55.7 \pm 0.7 \text{ cm}^{-1}$ . The anharmonicity of the  $B1$  state had been estimated elsewhere assuming the Morse potential and Morse’s approximation

$$D'_e = \frac{(\omega'_e)^2}{4\omega'_e x'_e} \quad (1)$$

and using experimental values  $D'_0$  and  $\omega'_0$  [7]. This treatment, which is evidently not appropriate in this case, gave  $\omega'_0 x'_0 = 0.4 \text{ cm}^{-1}$  and our present experimental data, when subjected to the same treatment, yielded  $\omega'_0 = 0.38 \text{ cm}^{-1}$ . The curvature of the Birge-Sponer plot in Fig. 2 leads to the dissociation limit  $v'_D = 9$  rather than  $v'_D = 22$ , which had been derived from a linear extrapolation [7], and indicates that the number of vibrational states con-

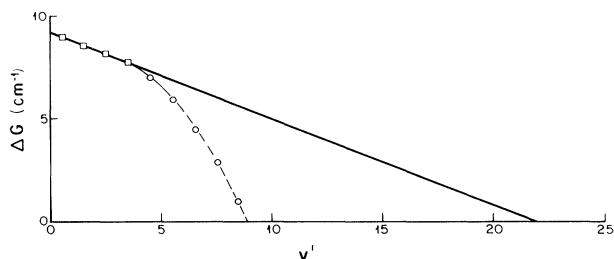


FIG. 2. A Birge-Sponer plot of the  $v'$  progression in the  $B1 \leftarrow X0^+$  excitation spectrum of CdKr, showing both “linear” ( $\square$ ) and actual ( $\circ$ ) extrapolation.

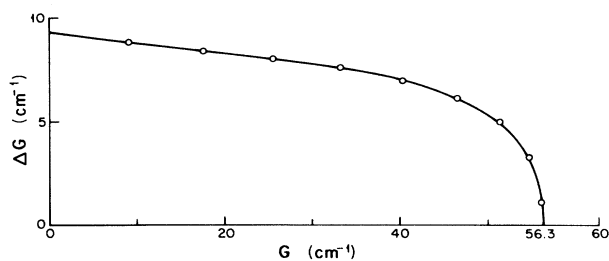


FIG. 3. A plot of  $\Delta G(v' + \frac{1}{2})$  against  $G(v')$  for the  $v'$  progression in the  $B1 \leftarrow X0^+$  spectrum of CdKr.

tained in the potential well and the anharmonicity  $\omega'_0 x'_0$  are very different from the values obtained from the conventional Birge-Sponer analysis.

We determined the anharmonicity of the  $B1$  state by using the experimentally found value  $D'_e$  and the Morse potential in an unconventional way. This was done by carrying out two computer simulations of the excitation spectrum. In the first, we used the difference  $r''_e - r'_e$  as an adjustable parameter and  $\omega'_e x'_e = 0.38 \text{ cm}^{-1}$  as a trial value. In the second simulation, we held  $r''_e - r'_e$  at its optimal value and adjusted  $\omega'_e x'_e$  to obtain the best fit to the experimental spectrum, which is shown in Fig. 4. The modeling calculation yielded  $\omega'_e x'_e \sim 0.26 \text{ cm}^{-1}$  and  $r'_e = 5.07 \text{ \AA}$ , which was obtained using  $r'_e(X0^+) = 4.5 \text{ \AA}$ , a value calculated with the aid of the London dispersion relation [15] and the experimentally determined  $D''_e$ . The resulting value  $r''_e - r'_e = 0.57 \text{ \AA}$  is also consistent with the observed degradation of the vibrational components towards longer wavelengths, which may be seen in Fig. 1.

#### B. The $A0^+ \leftarrow X0^+$ excitation spectrum

Figure 5 shows a trace of the excitation spectrum arising from the  $A0^+ \leftarrow X0^+$  vibronic transitions. The vibrational components are degraded towards shorter wavelengths, suggesting that  $r'_e(A0^+) < r''_e(X0^+)$ . The spec-

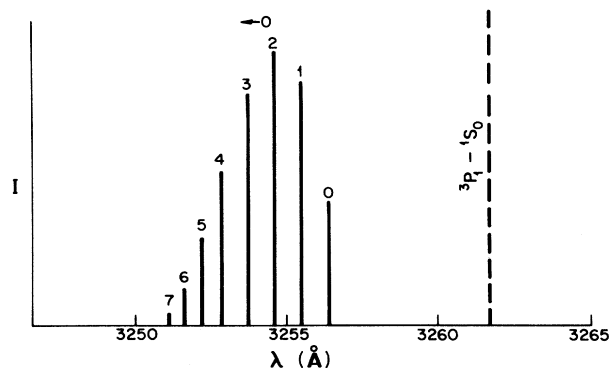


FIG. 4. Computer simulation of the  $B1 \leftarrow X0^+$  excitation spectrum of CdKr, showing relative intensities of the vibrational components.  $r''_e - r'_e$  was held at  $0.57 \text{ \AA}$  and the simulation yielded  $\omega'_e x'_e = 0.26 \text{ cm}^{-1}$ .

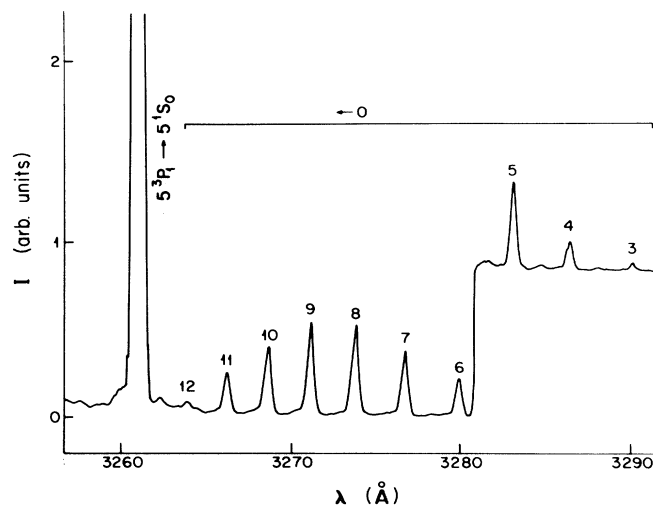


FIG. 5.  $A0^+ \leftarrow X0^+$  excitation spectrum showing a  $v'$  progression. The abrupt change in background level near  $3280 \text{ \AA}$  is due to a change in the amplification factor of the boxcar.

trum consists of a  $v'$  progression and the components are listed in Table II following the assignments given by Kvaran *et al.* [8], though we were able to record the  $v' = 3 \leftarrow v'' = 0$  band, which was not observed by these authors. Figure 6 shows a straightforward Birge-Sponer plot of the spectrum. Extrapolation of the straight line to  $v' = 0$  permitted the prediction of the frequencies of the

TABLE II. Frequencies of  $A0^+ \leftarrow X0^+$  vibrational bands. Asterisks indicate values obtained from extrapolation.

$v' \leftarrow v''$	$\tilde{\nu} \text{ (cm}^{-1}\text{)}$	$\Delta G(v') \text{ (cm}^{-1}\text{)}$
$0 \leftarrow 0$	30 281.3*	
$1 \leftarrow 0$	30 318.5*	37.2
$2 \leftarrow 0$	30 354.3*	35.8
$3 \leftarrow 0$	30 388.3	34.0
$4 \leftarrow 0$	30 421.5	33.2
$5 \leftarrow 0$	30 452.0	30.5
$6 \leftarrow 0$	30 481.1	29.1
$7 \leftarrow 0$	30 509.2	28.1
$8 \leftarrow 0$	30 536.3	27.1
$9 \leftarrow 0$	30 561.0	24.7
$10 \leftarrow 0$	30 584.5	23.5
$11 \leftarrow 0$	30 607.0	22.5
$12 \leftarrow 0$	30 628.0	21.0

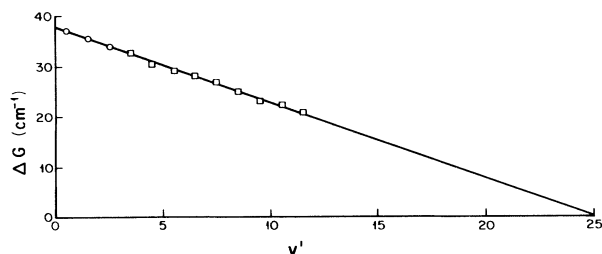


FIG. 6. A Birge-Spencer plot of the  $v'$  progression in the  $A0^+ \leftarrow X0^+$  spectrum of CdKr.

“missing”  $v'=0, 1,$  and  $2$  components, and yielded  $\omega'_0$  for the  $A0^+$  state.

The dissociation energy of the  $A0^+$  state was calculated using the relation

$$D'_0(A0^+) + \tilde{\nu}_{00}(A0^+ \leftarrow X0^+) = D''_0(X0^+) + \tilde{\nu}(^3P_1 \leftarrow ^1S_0) \quad (2)$$

in which the dissociation energy  $D''_0(X0^+)$  was obtained from the frequencies of the  $B1 \leftarrow X0^+$  hot bands and  $D'_0(B1)$ . The resulting value  $D'_0(A0^+) = 479 \text{ cm}^{-1}$  agrees exactly with  $D'_0$  obtained from the extrapolation of the Birge-Spencer plot in Fig. 6 to the dissociation limit  $v'=25.2$ . It is thus evident that the PE curve for the  $A0^+$  state may be satisfactorily represented by the Morse potential. This conclusion is further justified by the computer simulation of the  $A0^+ \leftarrow X0^+$  excitation spectrum, in which we calculated the Franck-Condon (FC) factors using the experimentally determined molecular constants in conjunction with the Morse potential [13] and varied the difference  $r'_e - r''_e$  to obtain the best fit; the simulated spectrum is shown in Fig. 7. In carrying out the computer-modeling procedure we found the intensity pattern to be sensitive also to variations in  $\omega'_e$  and  $\omega'_e x'_e$ , and tried various  $v'$  assignments of the spectral components obtaining the corresponding values  $\omega'_e$ . As the result of this exercise we were able to confirm unequivocally the assignments of the components reported by Kvaran *et al.* [8].

The computer simulation yielded  $r'_e - r''_e = -1.0 \text{ \AA}$ , which is consistent with the observed “blue-shading” (degradation towards shorter wavelengths) of the vibrational components. This result led to the estimate of  $r'_e = 3.5 \text{ \AA}$  for the  $A0^+$  state.  $r''_e$  for the  $X0^+$  ground state was also calculated using the London dispersion relation [15], the experimentally determined  $D''_e$  value, and the polarizabilities of Cd and Kr as suggested in Ref. [16], a method which we used previously with some success [1].

### C. The $X0^+$ ground state of CdKr

The intensities of the two hot bands indicated in Fig. 1 and Table I were monitored in relation to the  $X/D$  parameter whose decrease caused an increase in the frequency of collisions in the expanded beam and resulted in a corresponding increase in the hot-band intensity. The difference of the hot-band frequencies,  $9.0 \text{ cm}^{-1}$ , corre-

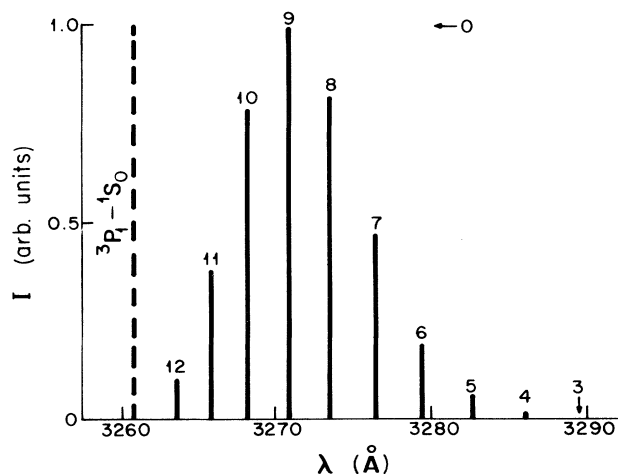


FIG. 7. Computer simulation of the  $A0^+ \leftarrow X0^+$  excitation spectrum showing relative intensities of the vibrational components.

sponds to the value  $8.9 \text{ cm}^{-1}$  for the energy interval between the  $v'=0$  and  $1$  vibrational levels of the  $B1$  state derived from the  $v'$  progression. These data also yield  $\omega''_0$  for the  $X0^+$  state:

$$\begin{aligned} \omega''_0 &= \tilde{\nu}_{00} - \tilde{\nu}_{01} \\ &= 30\,706.2 \text{ cm}^{-1} - 30\,689.0 \text{ cm}^{-1} \\ &= 17.2 \text{ cm}^{-1}. \end{aligned} \quad (3)$$

Using  $D'_0(B1)$  from Sec. III A and data from Tables I and II, we have

$$D'_0(B1) + \tilde{\nu}_{00}(B1 \leftarrow X0^+) = \tilde{\nu}(^3P_1 \leftarrow ^1S_0) + D''_0(X0^+), \quad (4)$$

which leads to

$$\begin{aligned} D''_0(X0^+) &= 55.6 \text{ cm}^{-1} + 30\,706.2 \text{ cm}^{-1} - 30\,656 \text{ cm}^{-1} \\ &= 105.8 \text{ cm}^{-1} \end{aligned} \quad (5)$$

and  $\omega''_0 x''_0 = 0.70 \text{ cm}^{-1}$  if the Morse potential is assumed for the  $X0^+$  state. The various spectroscopic constants, especially  $D''_0$  and  $D''_e$ , differ significantly from the values reported by Kowalski, Czajkowski, and Breckenridge [7] which were derived from measurements on a  $B1 \leftarrow X0^+$  spectrum containing fewer components than are shown in Fig. 1. The constants quoted in Refs. [8] and [17] were derived from the same measurement [7], but Bousquet's [18] estimate  $D''_e = 131 \pm 10 \text{ cm}^{-1}$  agrees with our value within the stated limits of error.

As mentioned above, we estimate the equilibrium internuclear separation in the  $X0^+$  ground state to be  $r''_e = -4.5 + 0.2 \text{ \AA}$  using the London dispersion relation [15]. This is significantly larger than the value  $r''_e = 3.55$  or  $3.63 \text{ \AA}$  calculated by Czuchaj and Sienkiewicz [5,9], who estimated it using empirical mixing rules and used it as the initial parameter for the calculation of the CdKr

PE curves. An alternative semiempirical result was obtained by Bousquet [18], who found  $r_e'' = 3.75 \pm 0.2$  Å. Some recent computer-modeling calculations of an excitation spectrum associated with the  $C^1\Pi_1$  state of CdKr [8,17] employed an arbitrary value  $r_e'' = 3.17$  Å chosen as most consistent with the measured  $r_e'' = 3.61$  and  $3.28$  Å for CdNe and CdAr, respectively. The computer simulation described in Refs. [8] and [17] yielded  $r_e'' - r_e' = 1.16$  Å and thus a value  $r_e''(XO^+) = 4.33$  Å, which was used to construct a PE curve for the ground state of CdKr [17]. It should be noted that the experimental data points obtained by Bousquet [18], who investigated the temperature dependence of light absorption by CdKr, can be fitted to the results of Funk, Kvaran, and Breckenridge [17] if Bousquet's data points are shifted by  $0.58$  Å towards larger values of  $r_e$ . This last result agrees with our findings within the stated limits of accuracy.

We have recently carried out additional (and more accurate) computer simulations of previously recorded CdNe and CdAr spectra [1], obtaining values for  $r_e'(AO^+)$  and  $r_e''(XO^+)$  that, as may be seen in Table III, are in excellent agreement with the values derived from direct measurements of the corresponding  $B_e'$  and  $B_e''$  rotational constants [8]. Data obtained from spectroscopic measurements on CdNe, CdAr, and CdKr indicate that the  $r_e$  values for these molecules are rather larger than those predicted by estimates derived from theoretical mixing rules [5,9] and are also larger than the semiempirical values suggested by Bousquet [18]. It would appear that the London dispersion relation [15] provides a reasonable means to estimate  $r_e''$  from spectroscopic data and to gain additional information on these van der Waals molecules.

#### D. Spectroscopic constants and PE curves for the $XO^+$ , $AO^+$ , and $B1$ states

The spectroscopic constants for the  $B1$ ,  $AO^+$ , and  $XO^+$  states in CdKr, obtained from the analysis of the spectra, are compared in Table IV with values reported elsewhere. The table includes both  $\omega_e'x_e'$  values of  $0.26$  and  $0.38$   $\text{cm}^{-1}$  for the  $B1$  state, which were used in the computer simulation described in Sec. III A. We also show in Fig. 8 the PE curves for the  $XO^+$  ground state and the lowest excited states asymptotic to the  $5^3P_0$  and

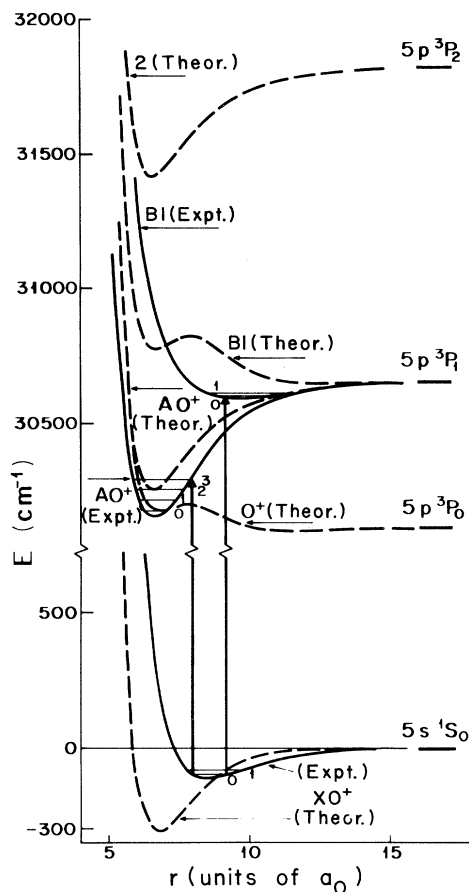


FIG. 8. A comparison of PE diagrams for CdKr obtained from our experimental data fitted to the Morse potential, and from theoretical calculations (Refs. [5] and [9]). —, experimental; ---, theoretical.

$5^3P_1$  Cd atomic states. The curves resulting from our experimental data are drawn according to the Morse approximation [13] and the theoretical curves were calculated by Czuchaj and Sienkiewicz [5,9] using Baylis's pseudopotentials [4]. As may be seen in Fig. 8, there is a considerable discrepancy between the theoretical and the experimental ground-state curves. The theoretical curve

TABLE III. Equilibrium internuclear separations in the  $AO^+$  and  $XO^+$  states of CdNe and CdAr (Å).

Designation	CdNe		CdAr	
	$AO^+$	$XO^+$	$AO^+$	$XO^+$
$r_e' - r_e''$	$-0.6 \pm 0.01^a$		$-0.85 \pm 0.01^a$	
$r_e'$	$3.50 \pm 0.2^a$		$3.45 \pm 0.2^a$	
	$3.62 \pm 0.05^b$		$3.45 \pm 0.03^b$	
$r_e''$		$4.1 \pm 0.2^a$		$4.3 \pm 0.04^a$
		$4.26 \pm 0.05^b$		$4.33 \pm 0.04^b$

<sup>a</sup>Obtained from the best fit of FC factors (calculated from the Morse potential) to the experimental data of Ref. [1].

<sup>b</sup>From Ref. [8].

TABLE IV. Spectroscopic constants for CdKr.

Designation	$B1$	$A0^+$	$X0^+$
$\omega_0''$ ( $\text{cm}^{-1}$ )			17.2; <sup>a</sup> 16.6 <sup>b</sup>
$\omega_0'$ ( $\text{cm}^{-1}$ )	9.2; <sup>a</sup> 10.3 <sup>c</sup>	38.0; <sup>a</sup> 37.1 <sup>d</sup>	
$\omega_0''x_0''$ ( $\text{cm}^{-1}$ )			0.70; <sup>a</sup> 1.14; <sup>c</sup> 0.58 <sup>d</sup>
$\omega_0'x_0'$ ( $\text{cm}^{-1}$ )	0.27; <sup>a</sup> 0.36; <sup>a</sup> 0.4 <sup>c</sup>	0.75; <sup>a</sup> 0.65 <sup>d</sup>	
$D_0''$ ( $\text{cm}^{-1}$ )			105.8; <sup>a</sup> 118 <sup>c</sup>
$D_0'$ ( $\text{cm}^{-1}$ )	55.6 <sup>a</sup>	479.4 <sup>a</sup>	
$D_e''$ ( $\text{cm}^{-1}$ )			114.4; <sup>a</sup> 129; <sup>c,d</sup> 310; <sup>e</sup> 131 <sup>f</sup>
$D_e'$ ( $\text{cm}^{-1}$ )	60.2; <sup>a</sup> 72 <sup>e</sup>	513; <sup>b</sup> 498.9 <sup>a</sup>	
$\omega_e''$ ( $\text{cm}^{-1}$ )			17.9; <sup>a</sup> 16.6 <sup>b</sup>
$\omega_e'$ ( $\text{cm}^{-1}$ )	9.3 <sup>a</sup>	38.6; <sup>a</sup> 37 <sup>d</sup>	
$\omega_e''x_e''$ ( $\text{cm}^{-1}$ )			0.70; <sup>a</sup> 0.58 <sup>b</sup>
$\omega_e'x_e'$ ( $\text{cm}^{-1}$ )	0.26; <sup>a</sup> 0.38 <sup>a</sup>	0.75; <sup>a</sup> 0.65 <sup>d</sup>	
$r_e' - r_e''$ ( $\text{\AA}$ )	0.57 <sup>a</sup>	1.00 <sup>a</sup>	
$r_e''$ ( $\text{\AA}$ )			4.5; <sup>a</sup> 4.33; <sup>b</sup> 3.63; <sup>c</sup> 3.75 <sup>f</sup>
$r_e'$ ( $\text{\AA}$ )	5.07 <sup>a</sup>	3.50; <sup>a</sup> 3.44 <sup>c</sup>	
$T_e'$ ( $\text{cm}^{-1}$ )	30 710.5 <sup>a</sup>	30 272.1 <sup>a</sup>	

<sup>a</sup>This work.

<sup>b</sup>Reference [17].

<sup>c</sup>Reference [7].

<sup>d</sup>Reference [8].

<sup>e</sup>References [5] and [9].

<sup>f</sup>Reference [18].

indicates  $r_e'' = 3.6 \text{ \AA}$  and  $D_e'' = 310 \text{ cm}^{-1}$  while the experimental curve indicates  $r_e'' = 4.5 \text{ \AA}$  and  $D_e'' = 114.4 \text{ cm}^{-1}$ . The discrepancy is much less dramatic for the  $A0^+$  state where the theoretical and experimental  $D_e'$  and  $r_e'$  values differ by 23% and 2%, respectively. The  $B1$  state appears to be weakly bound with  $D_e' = 60.2 \text{ cm}^{-1}$  and  $r_e' = 5.07 \text{ cm}^{-1}$ , while the theoretical calculation predicts an essentially repulsive state with a shallow well at an  $r_e$  value that is inconsistent with our experimental data. It is apparent from Fig. 8 that the relative positions on the  $r$  axis of the theoretically calculated PE minima of the  $B1$ ,  $A0^+$ , and  $X0^+$  states cannot be reconciled with the data obtained from our experiment. For example, the configuration of the calculated PE curves [5,9] suggests a relatively large FC factor for the  $v' = 0 \leftarrow v'' = 0$  ( $A0^+ \leftarrow X0^+$ ) transition, which, however, was not observed in our spectrum in which the first (and very faint) component corresponded to the  $v' = 3 \leftarrow v'' = 0$  transition.

No spectroscopic data have been reported for the  $0^-(5p^3P_0)$  state, which appears to constitute the only channel for the depopulation (quenching) of the  $\text{Cd}(5^3P_1)$  state by inelastic collisions with ground-state Cd and noble-gas atoms [5,9].

#### IV. SUMMARY AND CONCLUSIONS

$A0^+ \leftarrow X0^+$  and  $B1 \leftarrow X0^+$  excitation spectra of CdKr were produced in a supersonic expansion beam crossed with a laser beam. Analyses of the vibrational structures, reinforced by computer simulation of the spectra, yielded molecular constants including equilibrium internuclear separations for the three states, which are summarized in Table IV. The experimental data were used to construct PE curves for the  $X0^+$ ,  $A0^+$ , and  $B1$  states, which are compared in Fig. 8 with theoretical PE curves and clearly indicate the extent to which the theoretical curves are correct.

#### ACKNOWLEDGMENTS

This research was supported by the Natural Sciences and Engineering Research Council of Canada and by the Ontario Laser and Lightwave Research Centre.

- [1] R. Bobkowski, M. Czajkowski, and L. Krause, Phys. Rev. A **41**, 243 (1990).  
 [2] I. Wallace, R. R. Bennett, and W. H. Breckenridge, Chem. Phys. Lett. **153**, 127 (1988).  
 [3] R. R. Bennett and W. H. Breckenridge, J. Chem. Phys. **92**, 1588 (1990).

- [4] W. E. Baylis, J. Chem. Phys. **51**, 2665 (1969).  
 [5] E. Czuchaj and J. Sienkiewicz, J. Phys. B **17**, 2251 (1984).  
 [6] See, for example, D. H. Levy, Ann. Rev. Phys. Chem. **31**, 197 (1980), and references therein.  
 [7] A. Kowalski, M. Czajkowski, and W. H. Breckenridge, Chem. Phys. Lett. **119**, 368 (1985); **121**, 217 (1985).

- [8] A. Kvaran, D. J. Funk, A. Kowalski, and W. H. Breckenridge, *J. Chem. Phys.* **89**, 6069 (1988).
- [9] E. Czuchaj and J. Sienkiewicz (unpublished).
- [10] M. Czajkowski, R. Bobkowski, and L. Krause, *Phys. Rev. A* **40**, 4338 (1989).
- [11] W. Kedzierski, R. Berends, J. B. Atkinson, and L. Krause, *J. Phys. E* **21**, 796 (1988).
- [12] D. M. Lubman, C. T. Rettner, and R. N. Zare, *J. Chem. Phys.* **86**, 1129 (1982).
- [13] P. M. Morse, *Phys. Rev.* **34**, 57 (1929).
- [14] A. G. Gaydon, *Dissociation Energies* (Chapman and Hall, London, 1968).
- [15] F. London, *Z. Phys.* **63**, 243 (1930); *Z. Phys. Chem. B* **11**, 222 (1930).
- [16] T. M. Miller and B. Bederson, in *Advances in Atomic and Molecular Physics*, edited by D. R. Bates and B. Bederson (Academic, New York, 1977), Vol. 13.
- [17] D. Funk, A. Kvaran, and W. H. Breckenridge, *J. Chem. Phys.* **90**, 2915 (1989).
- [18] C. Bousquet, *J. Phys. B* **19**, 3859 (1986).